Proc. Natl. Acad. Sci. USA
Vol. 92, pp. 6334–6338, July 1995
Biochemistry

Three-dimensional structure of a cysteine-rich repeat from the low-density lipoprotein receptor

NORELLE L. DALY*, MARTIN J. SCANLON†, JULIANNE T. DJORDJEVIC*, PAULUS A. KROON*, AND ROSS SMITH*‡

*Centre for Protein Structure, Function and Engineering, Biochemistry Department, and †Centre for Drug Design and Development, The University of Queensland, Qld 4072, Australia

Communicated by Michael S. Brown, The University of Texas Southwestern Medical Center, Dallas, TX, March 28, 1995

ABSTRACT **The low-density lipoprotein (LDL) receptor plays a central role in mammalian cholesterol metabolism, clearing lipoproteins which bear apolipoproteins E and B-100 from plasma. Mutations in this molecule are associated with familial hypercholesterolemia, a condition which leads to an elevated plasma cholesterol concentration and accelerated atherosclerosis. The N-terminal segment of the LDL receptor contains a heptad of cysteine-rich repeats that bind the lipoproteins. Similar repeats are present in related receptors, including the very low-density lipoprotein receptor and the LDL receptor-related protein/α_2-macroglobulin receptor, and in proteins which are functionally unrelated, such as the C9 component of complement. The first repeat of the human LDL receptor has been expressed in *Escherichia coli* as a glutathione *S*-transferase fusion protein, and the cleaved and purified receptor module has been shown to fold to a single, fully oxidized form that is recognized by the monoclonal antibody IgG-C7 in the presence of calcium ions. The three-dimensional structure of this module has been determined by two-dimensional NMR spectroscopy and shown to consist of a β-hairpin structure, followed by a series of β turns. Many of the side chains of the acidic residues, including the highly conserved Ser-Asp-Glu triad, are clustered on one face of the module. To our knowledge, this structure has not previously been described in any other protein and may represent a structural paradigm both for the other modules in the LDL receptor and for the homologous domains of several other proteins. Calcium ions had only minor effects on the CD spectrum and no effect on the ^{1}H NMR spectrum of the repeat, suggesting that they induce no significant conformational change.**

The low-density lipoprotein (LDL) receptor regulates the concentration of plasma LDL and cholesterol by internalizing apolipoprotein (apo) B-100- and apoE-containing lipoproteins (1). These apolipoproteins are present in a variety of lipoproteins, including very low-density lipoprotein (VLDL) and intermediate-density lipoprotein; however, apoB-100 is the only protein constituent of LDL (2). Mutations in the LDL receptor are associated with familial hypercholesterolemia (3), in which the number of functional receptors is reduced, resulting in elevated concentrations of plasma LDL and cholesterol and leading to accelerated atherosclerosis (4). Five functionally discrete domains are present in the LDL receptor, including an epidermal growth factor-like domain and a heptad of cysteine-rich repeats that form the binding site for LDL (5). Different combinations of these repeats are involved in binding apo E and apoB-100 (6). Deletion of a single cysteine-rich repeat can alter the binding specificity of the receptor (7).

There is 40–50% sequence similarity between the repeats in the human LDL receptor ligand-binding domain, with each containing six cysteine residues and a highly conserved cluster of negatively charged amino acids (5). The lysine and arginine residues present in apoB-100 and apoE have been postulated to interact with these negatively charged amino acids (5, 8). In addition, it has been suggested that calcium ions interact with the repeats, as ligand binding is calcium dependent (9). The N-terminal cysteine-rich repeat of the LDL receptor (LB1) is not involved in binding the ligands; however, it appears to contain a calcium-binding site, as it is recognized by monoclonal antibody IgG-C7 only in the presence of calcium ions (9–11). This antibody was raised against the intact receptor and is conformation specific, as binding is abolished when the disulfide bonds of the repeat are reduced (10, 11).

A number of other proteins also contain these repeats, including the VLDL receptor (12), the LDL receptor-related protein/α_2-macroglobulin receptor (13), renal glycoprotein gp330 (14), the C9 component of complement (15), the linker protein of earthworm hemoglobin (16), and a receptor for subgroup A Rous sarcoma virus (17) (Fig. 1*A*). Within these repeats, the cysteine residues and C-terminal acidic residues are still highly conserved. As the repeats are present in a variety of unrelated proteins, it has been suggested that they are of ancient origin and may have been incorporated by exon shuffling (16).

LB1 has been expressed in *Escherichia coli* as a cleavable glutathione *S*-transferase fusion protein. Although LB1 is not involved in binding either ligand, it was initially chosen for study because of the availability of IgG-C7, which provides the best available assay for adoption of a native structure by the expressed protein. Given the level of amino acid sequence similarity between the repeats, it is likely that the first repeat will serve as a structural paradigm for the others. Thus, the three-dimensional structure of the recombinant LB1 peptide has been determined by NMR spectroscopy and shown to contain a previously undescribed structural motif comprising a short β-sheet segment at the N-terminal end, followed by a series of β-turns. The protein has a small core of hydrophobic residues and one face that bears many of the acidic side chains. The effect of calcium ions on the structure was also examined.§

MATERIALS AND METHODS

Expression and Purification. The cDNA of LB1 was amplified by PCR and cloned by insertion into the expression vector pGEX-2T (20). Recombinant LB1 was expressed as a thrombin-cleavable glutathione *S*-transferase fusion protein in *E. coli* by using a 15-liter Chemap (Männedorf, Switzerland)

The publication costs of this article were defrayed in part by page charge payment. This article must therefore be hereby marked "*advertisement*" in accordance with 18 U.S.C. §1734 solely to indicate this fact.

Abbreviations: apo, apolipoprotein; LDL, low-density lipoprotein; LB1, N-terminal cysteine-rich repeat of the LDL receptor; NOE, nuclear Overhauser enhancement; VLDL, very low-density lipoprotein.

‡To whom reprint requests should be addressed.

§The atomic coordinates have been deposited in the Protein Data Bank, Chemistry Department, Brookhaven National Laboratory, Upton, NY 11973 (reference 1LDL). The chemical shift data are available from the authors.

FIG. 1. Comparison of the amino acid sequences of LB1 from human (18) and *Xenopus* (19) LDL receptor (LDLR), human VLDL receptor (VLDLR) (12), the C9 component of complement (15), earthworm hemoglobin (Hb) (16), LDL receptor-related protein/α_2 macroglobulin receptor (LRP) (13), and renal glycoprotein gp330 (14) (*A*). Amino acids that are conserved at each site are boxed. The consensus sequence is shown at the bottom. (*B*) Sequence and disulfide connectivities of the protein used in the NMR studies. The N-terminal Gly-Ser results from the inclusion of a thrombin cleavage site in the fusion protein; these residues were not included in the structures depicted in Fig. 6 or in the numbering system used in the text.

fermentor. Following glutathione-agarose-affinity chromatography (20), the glutathione-agarose-bound glutathione *S*-transferase fusion protein was reduced by incubation with 1 mM dithiothreitol for 1 h at 37°C and cleaved with bovine thrombin (5 units per mg of fusion protein) to release recombinant LB1. Cleavage of the fusion protein with thrombin resulted in an extra two residues (glycine and serine) on the N terminus of LB1. In addition, the first four residues of the second repeat have also been included (Fig. 1*B*). The peptide was oxidized in the presence of 3 mM reduced and 0.3 mM oxidized glutathione and subsequently purified by reverse-phase HPLC on a C_{18} 8 mm × 100 mm Waters Radial-Pak column. Gradients of 0.1% aqueous trifluoroacetic acid and 0.1% trifluoroacetic acid in acetonitrile were employed with detection at 214 and 280 nm. Mass analysis was performed on a Sciex (Thornhill, ON, Canada) triple quadrupole mass spectrometer by using electrospray sample ionization. An estimate of free thiols in a 100-μg sample of HPLC-purified LB1 was obtained by using Ellman's reagent, 5,5′-dithiobis(2-nitrobenzoic acid) (21).

Monoclonal Antibody Analysis. HPLC-purified LB1 (4 μg) was dotted onto a 0.2-μm pore size nitrocellulose membrane. The membrane was baked for 8 h in a vacuum oven at 80°C and blocked for 1 h in Tris-buffered saline (20 mM Tris·HCl, pH 7.5/500 mM NaCl), which contained 5% (wt/vol) nonfat skim milk. Membranes were incubated with IgG-C7 in the presence or absence of 2 mM Ca^{2+}. Incubations in the absence of Ca^{2+} also contained 30 mM EDTA. Mouse monoclonal antibody IgG-C7 was prepared by injecting 6- to 11-week-old, BALB/c mice intraperitoneally with the IgG-C7-producing hybridoma CRL 1691, as described (22). Signals were detected by enhanced chemiluminescence substrate (Amersham) according to the manufacturer's instructions and exposed to x-ray film (Agfa) for time periods ranging from 5 s to 10 min.

Sedimentation Equilibrium. Sedimentation equilibrium experiments were performed on LB1 at 20°C by using a Beckman Optima XLA analytical ultracentrifuge. A pathlength of 2.51 mm was used with a homemade aluminium-filled epon centerpiece. The angular velocity was 60,000 rpm and the absorbance throughout the cell was recorded at 280 nm at 3-h intervals until equilibrium was attained. The molecular weight was determined by using a calculated partial specific volume of 0.687 ml/g.

CD Spectroscopy. Spectra were recorded on an Aviv Associates (Lakewood, NJ) model 62 DS spectrometer over the wavelength range of 260–190 nm and using a 0.1-mm pathlength cell, a bandwidth of 1.0 nm, a response time of 2 s, a scan rate of 20 nm·min^{-1}, and averaging over eight scans. The concentration of LB1 was 45 μM, and the pH was adjusted to 3.9 and 6.9 with 1 M NaOH. In addition, the effect of Ca^{2+} on the CD spectra was examined by adding a stoichiometric and 3-fold molar excess of calcium chloride.

NMR Spectroscopy. LB1 was dissolved in 10% ^2H_2O, pH 3.9 or pH 6.3, at a concentration of approximately 1 mM. For experiments in ^2H_2O, the sample was lyophilized and dissolved in 99.96% ^2H_2O (Wilmad, Buena, NY). The effect of calcium ions on the NMR spectra was also examined by adding a 3-fold molar excess of $CaCl_2$. ^1H NMR spectra were recorded on Bruker (Billerica, CA) model AMX 500 or ARX 500 spectrometers. Standard pulse sequences were used to obtain double quantum filtered correlated spectroscopy (DQF COSY) (23), total correlated spectroscopy (TOCSY) (24) (mixing times 80 and 100 ms), exclusive correlation spectroscopy (E.COSY) (25) and nuclear Overhauser enhancement (NOE) spectroscopy (NOESY) (26) (mixing times 65, 200, and 250 ms) spectra. The water signal was suppressed by low-power irradiation during the relaxation delay (2 s) and during the mixing time of the NOESY experiments. Two-dimensional experiments were generally collected into 4096 data points with 512 t_1 increments of 32–64 scans. Five TOCSY spectra collected with 16 scans and 128 t_1 increments and a relaxation delay of 1 s were interleaved with one-dimensional spectra for the ^2H_2O exchange experiments. Spectra were processed by using UXNMR (Bruker software). Generally, both dimensions were multiplied by a sine-bell function shifted by 90°, and a polynomial baseline correction was applied to selected regions. Spectra were recorded at pH 3.9 and 6.3, over a range of temperatures (290, 303, and 310 K) to enable assignment of overlapped resonances. Chemical shifts were referenced to external 3-trimethylsilylpropionic acid-d_4 (Fluka).

Structure Determination. A set of 55 structures was generated using 427 NOE distance restraints consisting of 200 intraresidue, 89 sequential, 64 short-range (≤5 residues), and 74 long-range (>5 residues) NOEs, which were classified as strong, medium, or weak and given upper bounds of 2.7, 3.5, and 5.0 Å, respectively. Peak volumes were measured in an NOESY spectrum recorded with a mixing time of 65 ms by using the EASY program (27) and used to derive distance restraints. Standard values of pseudoatom corrections were added (28). In addition, 1.5 Å was added to the upper distance limits for methyl protons, and degenerate methyl and methylene proton distances were multiplied by 1.2 and 1.1, respectively. The N-terminal glycine and serine had no distance restraints and were not included in the structure calculations. Torsional restraints were applied to seven ϕ angles with bounds of $-120° \pm 30°$ for angles with $^3J_{H^N-H^\alpha}$ coupling constants >9 Hz. An E.COSY experiment was used to estimate $^3J_{H^\alpha-H^\beta}$ coupling constants which were used in conjunction with NOE intensities to derive four χ_1 restraints.

The structures were generated on a Sun Microsystems (Mountain View, CA) model SPARCstation2 with *ab initio* simulated annealing using the XPLOR program (Version 3.1; Molecular Simulations, Waltham, MA), starting with a template and random ϕ and ψ angles. The simulated annealing protocol involved an initial energy minimization in a geometric force field (k_{bond} = 500 kcal·mol^{-1}·Å^{-2}, k_{ang} and $k_{improper}$ = 500 kcal·mol^{-1}·rad^{-2}) with a purely repulsive, nonbonded energy term (repel = 1, weight = 0.002), a soft square-well NOE-restraining function (k_{NOE} = 50 kcal·mol^{-1}·Å^{-2}, asymptote = 0.1), and an energy constant of 5 kcal·mol^{-1}·rad^{-2} for the

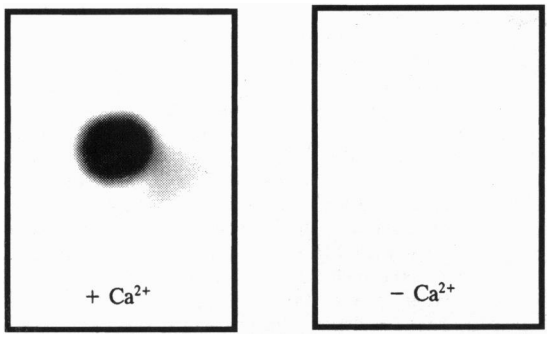

FIG. 2. LB1 was recognized by antibody IgG-C7 that binds to this repeat in the intact receptor but not to the unfolded polypeptide (10, 11). This immunoblot shows that the expressed LB1 binds the antibody only in the presence of calcium ions, just like the intact receptor.

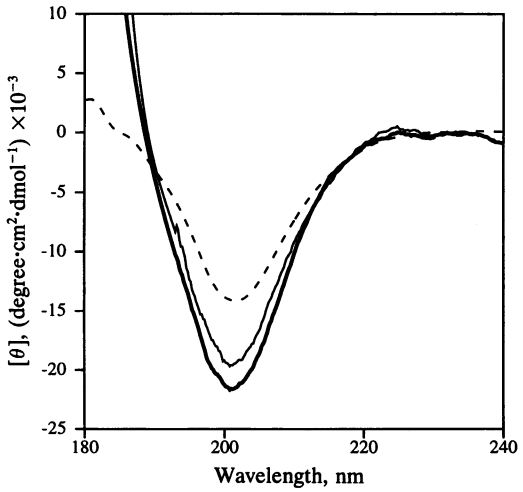

FIG. 3. CD spectra of LB1, 45 μM at pH 3.9 (dashed line), pH 6.9 (thin line), and pH 6.9 in the presence of 135 μM $CaCl_2$ (thick line). A stoichiometric or 3-fold molar excess of calcium chloride was added to the sample at pH 6.9. The stoichiometric concentration of calcium chloride had no effect (results not shown).

experimental dihedral angle restraints. A total of 30 ps of high temperature (1000 K) dynamics was carried out in two stages in which the van der Waals radii and weighting terms and NOE asymptote were varied. In the first 20 ps of dynamics, the weightings used were as follows: van der Waals, 0.002; angle, 0.4; and improper terms, 0.1. These weightings and the NOE asymptote were increased to 1 during the final 10 ps of high-temperature dynamics. Structures were then cooled to 100 K over 15 ps, during which the van der Waals radii and weighting were gradually changed to give final values of 0.8 and 4.0, respectively. The energy constant used for the experimental dihedral angle restraints was increased to 200 kcal·mol^{-1}·rad^{-2} for this step. Refinement of the structures was achieved with a second round of simulated annealing from

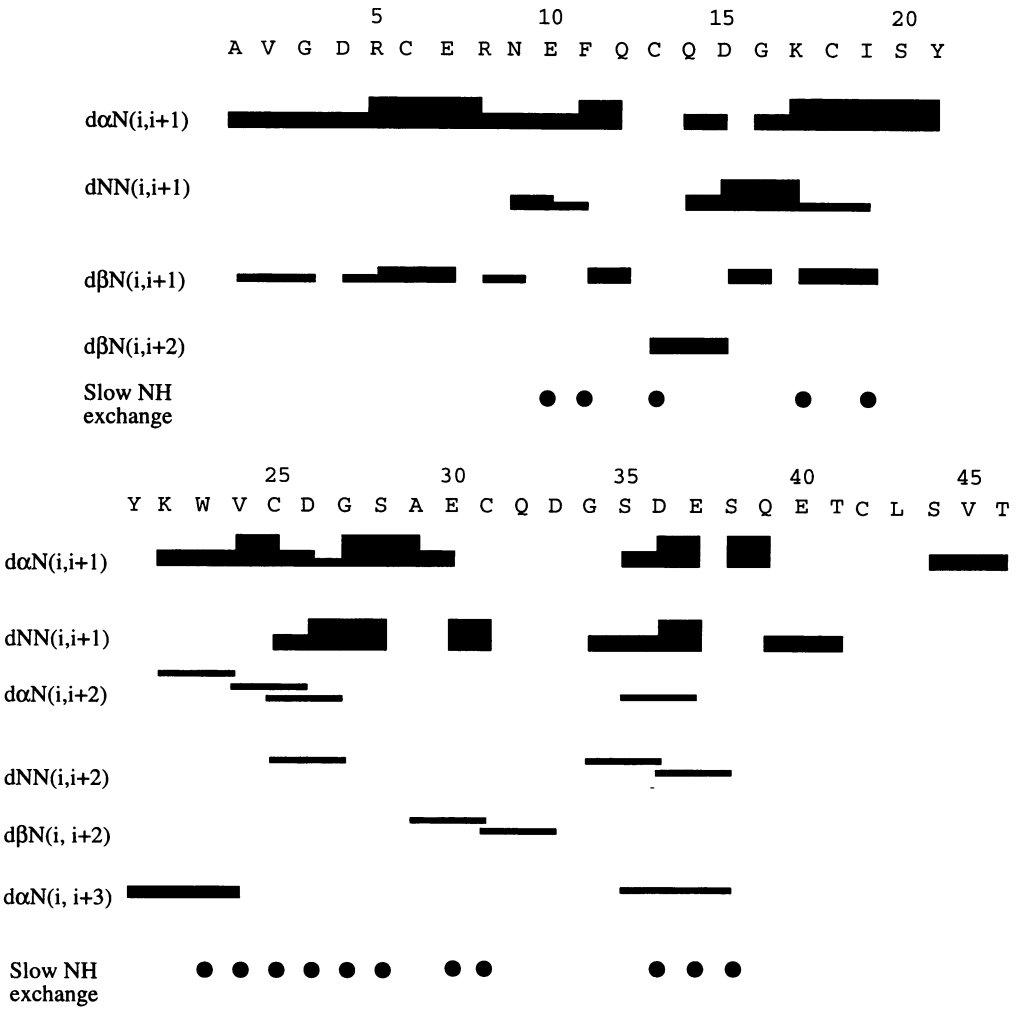

FIG. 4. Overview of short-range NOEs observed for LB1. The thickness of the lines corresponds to the intensity of NOEs. The filled circles indicate amide protons present 2.5 h after LB1 was dissolved in ^2H_2O.

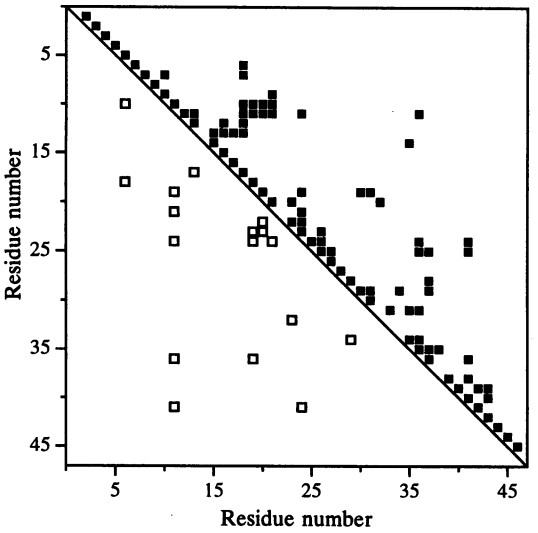

FIG. 5. Diagonal plot of the interresidue NOE distance restraints. The filled squares represent restraints involving at least one backbone atom, and the open squares indicate restraints involving only side-chain atoms.

1000 K to 100 K over 10 ps by using a square-well NOE-restraining function (k_{NOE} = 50 kcal·mol^{-1}·Å^{-2}) and an energy constant of 200 kcal·mol^{-1}·rad^{-2} for the experimental dihedral angle restraints. During the initial structure calculations, the disulfide connectivities were not explicitly defined; however, these calculations resulted in an unambiguous assignment of the disulfide bonds, which were then included as conformational restraints in the final subsequent simulated annealing and refinement calculations.

RESULTS AND DISCUSSION

Purified, oxidized LB1 migrates as a single symmetrical peak on isocratic HPLC (24:1 CH_3CN), indicating that only one of the possible disulfide bonding patterns is present. It appears to be fully oxidized as it does not react with Ellman's reagent, iodoacetamide, or vinylpyridine in the presence of denaturants (S. Bieri, J.T.D., N.L.D., R.S., and P.A.K., unpublished data). The conformation-specific antibody, IgG-C7, recognizes purified LB1, indicating that it is correctly folded (Fig. 2).

The CD spectra of LB1 in aqueous solution are indicative of a lack of regular secondary structure (Fig. 3). Minor changes occur in the CD spectra upon the addition of $CaCl_2$; however, no change was observed in the NMR spectra recorded in the presence of a 3-fold molar excess of $CaCl_2$. There is evidence suggesting that LB1 binds calcium (9); however, under the present conditions, calcium ions do not appear to induce a significant conformational change. Similarly, no substantial conformational changes were apparent in the NMR spectra over the pH range 3.9–6.9.

The resonance assignments and interproton distance constraints were obtained by conventional methods (29). Several α chemical shifts were below the water resonance; however, changing the pH and temperature shifted the overlapped resonances sufficiently to allow assignment of resonances to all residues except the N-terminal glycine. Although the CD spectra indicated the absence of ordered secondary structure, the amide shifts were well dispersed over 3 ppm, showing the presence of persistent three-dimensional structure. Structures were calculated from the spectra recorded at pH 6.3 and 303 K. The NOE restraints used in the final calculations are depicted in Figs. 4 and 5. The slowly exchanging amide proton resonances are also presented in Fig. 4.

Initial structures derived from NMR data without including the disulfide bonds as structural restraints revealed the follow-

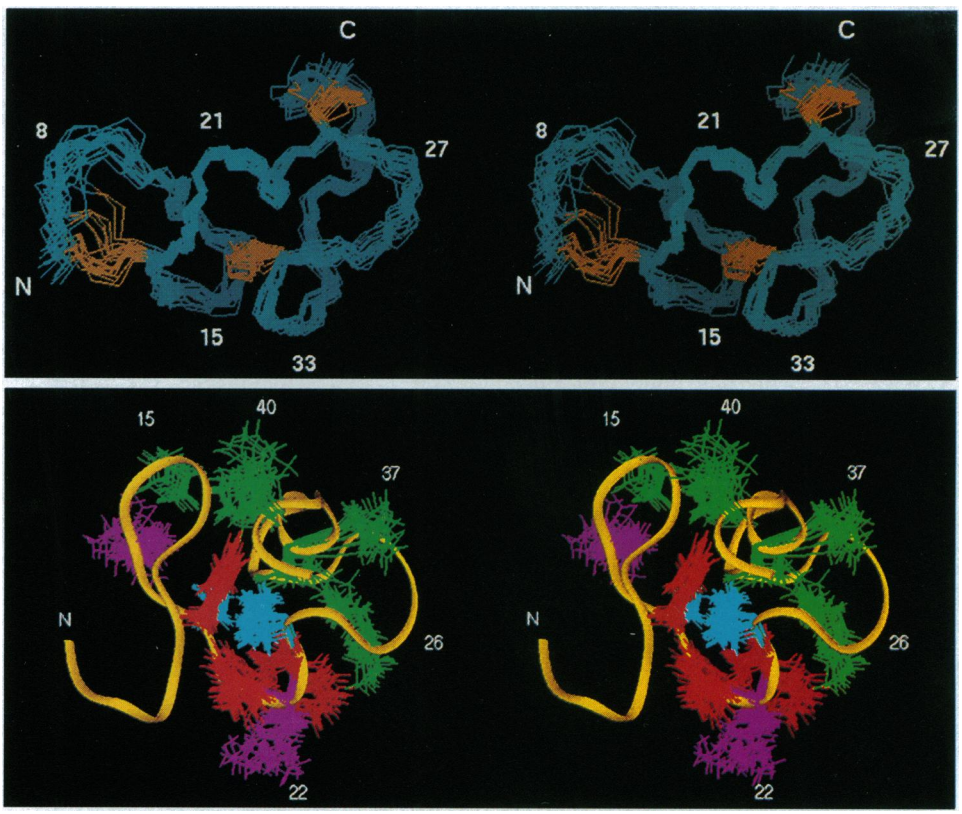

FIG. 6. Stereoview of the backbone (N, C$^{\alpha}$, C′) of 20 NMR-derived structures (residues 6–42) of the N-terminal LDL receptor ligand-binding repeat, superimposed over residues 11–42. The disulfide bonds are presented in orange/yellow (*Upper*). The side chains of acidic residues (Asp-15, Asp-26, Glu-30, Asp-33, Asp-36, Glu-37, and Glu-40) are highlighted in green, aromatic residues in red, Ile-19 and Val-24 in blue, and Lys side chains in pink (*Lower*).

ing pairings: Cys-6 Cys-18, Cys-13 Cys-31, and Cys-25 Cys-42. These connectivities were confirmed by a combination of partial reduction and alkylation and trypsin or proteinase K proteolysis, coupled with N-terminal sequencing and electrospray mass spectrometry (S. Bieri, J.T.D., N.L.D., R.S., and P.A.K., unpublished data).

In the final set of 55 structures generated with disulfide bond restraints, the 20 lowest-energy structures were selected for analysis. In these structures no NOE distance restraint was violated by >0.4 Å, and no angle restraints were violated by >4°. The root-mean-square deviation (RMSD) values from the experimental restraints and idealized geometry were as follows: NOE restraints, 0.05 ± 0.02 Å; dihedral restraints, 0.85° ± 0.2°; bonds, 0.0045 ± 0.0002 Å; angles, 0.50° ± 0.04°; and improper angles, 0.34° ± 0.03°. Energies corresponding to NOE restraints and dihedral restraints were 65 ± 4 kcal·mol^{-1} and 0.43 ± 0.2 kcal·mol^{-1}, respectively. The RMSD about the mean coordinate positions for residues Phe-11 to Cys-42 was 0.65 ± 0.14 Å for heavy atoms and 1.11 ± 0.12 Å for all atoms (Fig. 6 *Upper*).

Inspection of the low-energy structures revealed that residues Glu-10 to Ser-20 form a class three, three-residue β-hairpin structure (30), within which Phe-11, Asn-13, Lys-17, and Ile-19 have amide protons that exchange slowly and therefore appear to be involved in hydrogen bonds. This is followed by three β turns (31) involving residues Tyr-21 to Val-24, Ser-35 to Ser-38, and Gln-39 to Cys-42. The amide protons of residues Val-24 and Ser-38 exchange slowly and thus also appear to be involved in hydrogen bonds; however, Cys-42 is not. Additional turns are present from residues Cys-25 to Ser-28 and Cys-31 to Gly-34; however, these regions of the molecule are less well defined. The N- and C-terminal segments have few constraints and are thus poorly defined.

The residues Phe-11 and Ile-19, which are completely conserved between repeats in the LDL receptor, together with Tyr-21, Trp-23, and Val-24, form a hydrophobic cluster that is partly solvent-exposed. Despite this exposure of the hydrophobic core, the peptide showed no sign of aggregation at near millimolar concentrations in sedimentation equilibrium experiments, which gave M_r = 5200 ± 200, or in the NMR spectra. The content of hydrophobic residues in LB1 is far lower than that in most globular proteins, and the core is consequently small. The side chains of the remaining hydrophobic residues, Leu-43 and Val-45, have poorly defined positions in the isolated repeat but would normally be present in the second cysteine-rich repeat of the LDL receptor.

The level of homology within the LDL receptors of several species (19) is higher than between the proteins listed in Fig. 1*A*. A consensus sequence of A-----C--RNEF-C-D--GKCI--KWVCDGS-EC-DGSDE--ETC (with some minor and generally conservative substitutions) spans the LB1 modules of human, rat, rabbit, hamster, and *Xenopus*, and a sequence of C-----F-C------CI-----C----(D/E)C---SDE----C is common to the seven repeats of the human receptor. The degree of conservation is higher across species for a given repeat than between repeats for a given species, suggesting distinct functions for the individual modules. However, in both of these consensus sequences, there is a cluster of acidic residues in the C-terminal half, which for LB1 includes Asp-26, Glu-30, Asp-33, Asp-36, Glu-37, and Glu-40. The carboxylates of Asp-26 and Glu-30 and of Asp-15 and Asp-33 lie close to each other; however, the latter pair of acidic residues are also in the vicinity of the basic side chain of Lys-17. In contrast, the carboxylate of Asp-36 is buried. The reason for the noninvolvement of LB1 in binding is unknown but may be related to the burying of the Asp-36 residue side chain, which is highly conserved and is thought to interact with the lipoproteins. Asp-15, Asp-26, Glu-30, Asp-33, and Glu-37 all appear on one face of the module, as shown in Fig. 6 *Lower*. This pattern, if repeated in the other domains, would form an appropriately charged surface for interaction with the basic residues of apo B-100 and apoE (5, 8).

A computerized search of structures lodged with the Protein Data Bank detected no other proteins with a comparable topology (32). Those having the closest structural homology had root-mean-square deviations of over 3.5 Å for the α-carbon atoms, matched only by aligning several short nonsequential segments, and bore no similarity in amino acid sequence to LB1. Thus, the topology of this module appears to be distinct from any other in the protein data base and is likely to be mimicked within the LDL receptor and in the other diverse proteins containing these cysteine-rich repeats.

We thank Dr. Ian Brereton for assistance with the NMR experiments; Dr. Liisa Holm, European Molecular Biology Laboratory, Heidelberg, for conducting the three-dimensional structure comparison; Dr. G. Ralston, University of Sydney, and Mr. M. Jacobsen, University of Queensland, for the sedimentation data; and Mr. S. Bieri for unpublished information on the disulfide bond connectivities. This research was supported by a grant from the Australian National Health and Medical Research Council.

1. Goldstein, J. L., Anderson, R. G. W. & Brown, M. S. (1979) *Nature (London)* **279,** 679–685.
2. Mahley, R. W. & Innerarity, T. L. (1983) *Biochim. Biophys. Acta* **737,** 197–222.
3. Brown, M. S. & Goldstein, J. L. (1986) *Science* **232,** 34–47.
4. Goldstein, J. L. & Brown, M. S. (1983) in *The Metabolic Basis of Inherited Disease*, eds. Stanbury, J. B., Wyngaarden, J. B., Frederickson, D. S., Goldstein, J. L. & Brown, M. S. (McGraw-Hill, New York), pp. 672–712.
5. Yamamoto, T., Davis, C. G., Brown, M. S., Schneider, W. J., Casey, M. L., Goldstein, J. L. & Russell, D. W. (1984) *Cell* **39,** 27–38.
6. Hobbs, H. H., Brown, M. S., Goldstein, J. L. & Russell, D. W. (1986) *J. Biol. Chem.* **261,** 13114–13120.
7. Esser, V., Limbird, L. E., Brown, M. S., Goldstein, J. L. & Russell, D. W. (1988) *J. Biol. Chem.* **263,** 13282–13290.
8. Knott, T. J., Rall, J. S. C., Innerarity, T. L., Jacobson, S. F., Urdea, M. S., Levy-Wilson, B., Powell, L. M., Pease, R. J., Eddy, R., Nakai, H., Byers, M., Priestley, L. M., Robertson, E., Rall, L. B., Betsholtz, C., Shows, T. B., Mahley, R. W. & Scott, J. (1985) *Science* **230,** 37–43.
9. van Driel, I. R., Goldstein, J. L., Südhof, T. C. & Brown, M. S. (1987) *J. Biol. Chem.* **262,** 17443–17449.
10. Beisiegel, U., Schneider, W. J., Goldstein, J. L., Anderson, R. G. W. & Brown, M. S. (1981) *J. Biol. Chem.* **256,** 11923–11931.
11. Daniel, T. O., Schneider, W. J., Goldstein, J. L. & Brown, M. S. (1983) *J. Biol. Chem.* **258,** 4606–4611.
12. Sakai, J., Hoshino, A., Takahashi, S., Miura, Y., Ishii, H., Suzuki, H., Kawarabayasi, Y. & Yamamoto, T. (1994) *J. Biol. Chem.* **269,** 2173–2182.
13. Herz, J., Hamann, U., Rogne, S., Myklebost, O., Gausepohl, H. & Stanley, K. K. (1988) *EMBO J.* **7,** 4119–4127.
14. Raychowdhury, R., Niles, J. L., McCluskey, R. T. & Smith, J. A. (1989) *Science* **244,** 1163–1165.
15. Discipio, R. G., Gehring, M. R., Podack, E. R., Chen Kan, C., Hugli, T. E. & Gey, G. H. (1984) *Proc. Natl. Acad. Sci. USA* **81,** 7298–7302.
16. Suzuki, T. & Riggs, A. (1993) *J. Biol. Chem.* **268,** 13548–13555.
17. Bates, P., Young, J. A. T. & Varmus, H. E. (1993) *Cell* **74,** 1043–1051.
18. Südhof, T. C., Goldstein, J. L., Brown, M. S. & Russell, D. W. (1985) *Science* **228,** 815–822.
19. Mehta, K. D., Chen, W., Goldstein, J. L. & Brown, M. S. (1991) *J. Biol. Chem.* **266,** 10406–10414.
20. Smith, D. B. & Johnson, K. S. (1988) *Gene* **67,** 31–40.
21. Riddles, P. W., Blakeley, R. L. & Zerner, B. (1983) *Methods Enzymol.* **91,** 49–60.
22. Ausubel, F. M., Brent, R., Kingston, R. E., Moore, D. D., Seidman, J. G., Smith, J. A. & Struhl, K. (1993) *Current Protocols in Molecular Biology* (Wiley, New York).
23. Rance, M. (1987) *J. Magn. Reson.* **74,** 557–564.
24. Braunschweiler, L. & Ernst, R. R. (1983) *J. Magn. Reson.* **53,** 521–528.
25. Griesinger, C., Sorensen, O. W. & Ernst, R. R. (1986) *J. Chem. Phys.* **85,** 6837–6852.
26. Jeener, J., Meier, B. H., Bachmann, P. & Ernst, R. R. (1979) *J. Chem. Phys.* **71,** 4546–4553.
27. Eccles, C., Güntert, P., Billeter, M. & Wüthrich, K. (1991) *J. Biomol. NMR* **1,** 111–130.
28. Wüthrich, K., Billeter, M. & Braun, W. (1983) *J. Mol. Biol.* **169,** 949–961.
29. Wüthrich, K. (1986) *NMR of Proteins and Nucleic Acids* (Wiley, New York).
30. Milner-White, E. J. & Poet, R. (1987) *Trends Biochem. Sci.* **12,** 189–192.
31. Wilmot, C. M. & Thornton, J. M. (1990) *Protein Eng.* **3,** 479–493.
32. Holm, L. & Sander, C. (1993) *J. Mol. Biol.* **233,** 123–138.